Saudi Journal of Biological Sciences 28 (2021) 5684–5692

Contents lists available at ScienceDirect

Saudi Journal of Biological Sciences

journal homepage: www.sciencedirect.com

Original article

Inorganic polyphosphate from the immunobiotic *Lactobacillus rhamnosus* CRL1505 prevents inflammatory response in the respiratory tract

María A. Correa Deza, Antonieta Rodríguez de Olmos, Nadia E. Suárez, Graciela Font de Valdez, Susana Salva *, Carla L. Gerez

Centro de Referencia para Lactobacilos (CERELA), Consejo Nacional de Investigaciones Científicas y Técnicas (CONICET), San Miguel de Tucumán, Tucumán, Argentina

ARTICLE INFO

Article history:
Received 12 June 2020
Revised 31 May 2021
Accepted 2 June 2021
Available online 10 June 2021

Keywords:
Lactobacillus
Immunobiotic
Inorganic polyphosphate
Respiratory inflammation
TLR4
Innate immunity

ABSTRACT

Lactobacillus (L.) rhamnosus CRL1505 accumulates inorganic polyphosphate (polyP) in its cytoplasm in response to environmental stress. The aim of this study was to evaluate the potential effects of polyP from the immunobiotic CRL1505 on an acute respiratory inflammation murine animal model induced by lipopolysaccharide (LPS).

First, the presence of polyP granules in the cytoplasm of CRL1505 strain was evidenced by specific staining. Then, it was demonstrated in the intracellular extracts (ICE) of CRL1505 that polyP chain length is greater than 45 phosphate residues. In addition, the functionality of the genes involved in the polyP metabolism (*ppk*, *ppx1* and *ppx2*) was corroborated by RT-PCR. Finally, the possible effect of the ICE of CRL1505 strain containing polyP and a synthetic polyP was evaluated *in vivo* using a murine model of acute lung inflammation. It was observed that the level of cytokines pro-inflammatory (IL-17, IL-6, IL-2, IL-4, INF-γ) in serum was normalized in mice treated with ICE, which would indicate that polyP prevents the local inflammatory response in the respiratory tract. The potential application of ICE from *L. rhamnosus* CRL1505 as a novel bioproduct for the treatment of respiratory diseases is one of the projections of this work.

1. Introduction

Probiotic lactobacilli are microorganisms with health-promoting capacities on the host by different mechanisms such as enhancement of epithelial barrier function and modulation of immune response. Most of them are due to the interaction between the host cells and extracellular or intracellular components produced by the probiotic bacteria. Exopolysaccharides, bacteriocins, surface-associated and extracellular proteins/peptides as well as lipoteichoic acid are examples of well-known bioactive components from probiotics (Menard et al., 2004; Yan et al., 2007; Ewaschuk et al., 2008; Heuvelin et al., 2009; Petrof et al., 2009).

These beneficial bacteria and or their bioactive components are an interesting alternative as supplementary treatments for respiratory diseases (Dumas et al., 2018; Liu et al., 2018; Libertucci and Young, 2019). Acute respiratory diseases (ARDs) are infectious diseases that can affect the respiratory upper tract and even the lungs in more severe cases thus causing damage due to excessive inflammatory response. Mild cases of ARDs are treated with antibiotics, antivirals and anti-inflammatory drugs such as glucocorticoids. Intranasal drug administration is the most appropriate route for corticosteroids administration due to its rapid absorption and systemic distribution, fluticasone propionate and budesonide being the most frequently used despite some adverse effects, e.g., risk of dysphonia, oral candidiasis and cough.

Lactobacillus (*L.*) *rhamnosus* CRL1505 (CRL1505) is a widely studied probiotic strain (Salva et al., 2010; Kitazawa and Villena, 2014; Villena et al., 2016; Zelaya et al., 2016) that has been successfully transferred to the dairy industry in Argentina within the frame mark of social projects (Villena et al., 2012b). This strain improves the immune responses in the gut and beyond the gastrointestinal tract in mice (Salva et al., 2010) as well as in children attending pre-school daycare community centers (Villena et al., 2012b). Besides, CRL1505 also has protective effect against bacte-

* Corresponding author at: Chacabuco 145, 4000 Tucumán, Argentina.
E-mail address: ssalva@cerela.org.ar (S. Salva).

Peer review under responsibility of King Saud University.

Production and hosting by Elsevier

https://doi.org/10.1016/j.sjbs.2021.06.010
1319-562X/

rial respiratory pathogens using nasal administration in mice model (Herrera et al., 2014). In addition, changes induced by nasal administration of *L. rhamnosus* CRL1505 in the respiratory tract, increased resistance to infection with Respiratory Syncytial Virus (Chiba et al., 2013; Tomosada et al., 2013) and Influenza Virus (Zelaya et al., 2014; Zelaya et al., 2015; Tonetti et al., 2020). Recently, the beneficial effect of CRL1505 on respiratory immunity using model of acute lung inflammation triggered by the activation of TLR3 was demonstrated (Clua et al., 2017). Also, nasal immunocompetent adult mice challenged with LPS showed that soluble factors of *Lactobacillus reuteri* CRL1098 can modulate pro-inflammatory cytokine production and recruitment of immune cells to the airways and reduce the inflammatory tissue damage (Griet et al., 2014). These researches show that immunobiotic CRL1505 can be used as an interesting alternative to modulate the immune response in the respiratory tract in inflammatory diseases.

In the last decade, studies on probiotics (Villena et al., 2009; Kolling et al., 2015) support evidences of non-viable immunobiotics stimulating the immune system. This is the start point for developing novel bioproducts mainly for immunocompromised hosts (Markowicz et al., 2015) since it is possible to have beneficial effects regardless the cell viability that is an imperative requirement for probiotic products. In this sense, the peptidoglycan of CRL1505 is able to preserve the immunomodulatory capacity of non-viable CRL1505 (Kolling et al., 2015). In addition, recently it was demonstrated that CRL1505 may also accumulate inorganic polyphosphate (polyP) in the cytoplasm in response to environmental stress (Deza et al., 2017). These polyanions granules derived from probiotic strains have anti-inflammatory effects in inflammatory murine models as it was recently reported (Kashima et al., 2015; Tanaka et al., 2015).

From the above, the aim of this study was to evaluate the potencial effects of polyP accumulated by the immunobiotic CRL1505 on an acute respiratory inflammation murine animal model induced by lipopolysaccharide (LPS), for which the polyP granules in the cytoplasm of CRL1505 were quantified and it was estimated their molecular weight. Finally, the genes involved in polyP metabolism were evidenced in CRL1505.

2. Materials and methods

2.1. Microorganism and culture conditions

L. rhamnosus CRL1505 was obtained from the culture collection of Centro de Referencia para Lactobacilos (CERELA-CONICET, San Miguel de Tucumán, Tucumán, Argentina). The strain was grown in MCM broth (Deza et al., 2017) at 37 °C for 20 h, under free pH conditions and without agitation.

2.2. Visualization of polyP by Neisser staining

Smears of *L. rhamnosus* CRL1505 cultures were air-dried on clean and degreased slides and stained with Neisser's solution (Sigma-Aldrich Co, St. Louis, MO, United States), which specifically reveals the presence of inorganic polyP granules (Gurr, 1965; Alcántara et al., 2014). The granules were observed with an optical microscope (CX, Olympus, Tokyo, Japan) using an immersion objective (100×).

2.3. Electrophoresis of polyP in polyacrylamide gels (PAGE)

Intracellular extract (ICE) of *L. rhamnosus* CRL1505 obtained from active cultures was prepared for PAGE visualization. The pellet was recovered by centrifugation (10,000*g*, 15 min) and mixed with glass beads (150–212 μm diameter, Sigma-Aldrich Co, St. Louis, MO, United States) with a pellet:bead ratio 1:1 (w/w). Then, the cells were disrupted with a Mini-Bead Beater-8 cellular disruptor (Biospec Products Inc., Bartlesville, OK, United States) at maximum speed using 7 cycles of 1.5 min each, and ice intervals of 1 min between cycles. The cell debris and glass beads were removed by centrifugation (14,500*g*, 5 min, and 4 °C) and the ICE obtained was kept at −20 °C until used.

The polyP size of CRL1505 was determined in the ICE with the method of Leitão et al. (1995) with minor modifications. Briefly, 20 μL of ICE were mixed with the seed dye [Tris-Borate-EDTA buffer (5×, TBE): 90 mM Tris; 90 mM Borate; 2.7 mM EDTA; 5% glycerol; 0.01% bromine blue phenol and 0.02% xylene cyanol; pH 8.3] and loaded on 4% polyacrylamide gels (acrylamide:bisacrylamide ratio 20:1). The gels were run in TBE buffer (1×) and stained with a solution of toluidine blue (0.05%) in 25% methanol. A polyP standard composed of 45 phosphate residues (polyP 45; MW: 4748 Da; Sigma-Aldrich Co, St. Louis, MO, United States) was used as molecular size marker. This technique uses toluidine blue as basic staining dye for polyP. MCM broth medium was included to avoid interferences with other polyanions that may be present and also react with toluidine blue, as well as the culture supernatant (SN) of CRL 1505 to determine the presence of polyP in the extracellular medium as it was reported for *L. paracasei* JCM 1163 (Saiki et al., 2016)

2.4. Quantification of polyP as soluble phosphate

A spectrophotometric technique to quantify intracellular polyP was developed. Stationary phase cultures of *L. rhamnosus* CRL1505 were used for obtaining the ICE, which was treated with 1 M HCl at 100 °C for 30 min to hidrolized the polyP and release the orthophosphates molecules that form this polyanion. The soluble phosphate released was quantified by a spectrophotometric technique, according to De Angelis et al. (2003) and Smith et al. (2010). Briefly, 100 μL of ICE were mixed with 100 μL of a color reagent, formed by 80% solution A [1.5% (w/v) ammonium molybdate and 5.5% (v/v) acid sulfuric] and 20% solution B [2.7% (w/v) ferrous sulphate]. Samples were incubated at room temperature for 20 min and the absorbance was subsequently measured at 700 nm in a microplate reader (VERSA max, Molecular Devices, USA). Phosphate concentration was determined by reference to a standard curve using Na_2HPO_4 (2 mg/mL) (Figure Supplementary Fig. 1). The results were expressed as intracellular phosphate content in CRL1505 ICE (mg Na_2HPO_4/mL of extract).

2.5. Transcriptional analysis of coding genes for PPX1, PPX2 and PPK enzymes

Ppk, *ppx1* and *ppx2* encoding a polyphosphate kinase (PPK) and two exopolyphosphatases (PPX1 and PPX2, respectively), which are involved in the polyP metabolism of lactic acid bacteria (Alcántara et al., 2014). Total RNA isolation of CRL1505 (culture in MCM broth at 37 °C for 20 h, under free pH) was performed according to Raya et al. (1998). The isolated RNA was treated with the TURBO-free DNA™ kit (Ambion®, Invitrogen, Buenos Aires, Argentina) according to the manufacturer's instructions before cDNA synthesis. The cDNA synthesis was performed from 5 μg of total DNA-free RNA using the SuperScript™ III First-Strand Synthesis System kit (Invitrogen, Thermo Fisher Scientific, Buenos Aires, Argentina). The primers used in the RT-PCR are listed in Table 1. These were designed according to the *ppx1*, *ppx2* and *ppk* sequences in the genome of *L. rhamnosus* GG (NCBI Reference Sequence: NC_013198.1) and CRL 1505 (GenBank N°: ATBI00000000.1) with the First Quest program (Integrated DNA Technologies, Inc.). The RT-PCR reactions were performed in dupli-

Table 1
Primers used in PCR reactions for the identification of the *ppk*, *ppx1*, and *ppx2* genes.

Gen	Primer	Sequence 5′ → 3′	Tm (°C)	Product Lenght (bases)
Polyphosphate kinase	ppk-Foward	ATGCGGCTGTGTTCCAGTAA	51,78	898 bp
	ppk-Reverse	TCACGGCCCGATTGATTTGA	51,78	
Expolyphosfatase 1	ppx1-Foward	ATTCACGGCTCGGGTGTTC	53,25	909 bp
	ppx1-Reverse	AGGTAGCAACTCTGCACGAA	51,78	
Exopolyphosfatase 2	ppx2-Foward	GAATCTTTTGCTGCCGCGAT	51,78	881 bp
	ppx2-Reverse	ACCGTTGCGGGTGTATGAAA	51,78	

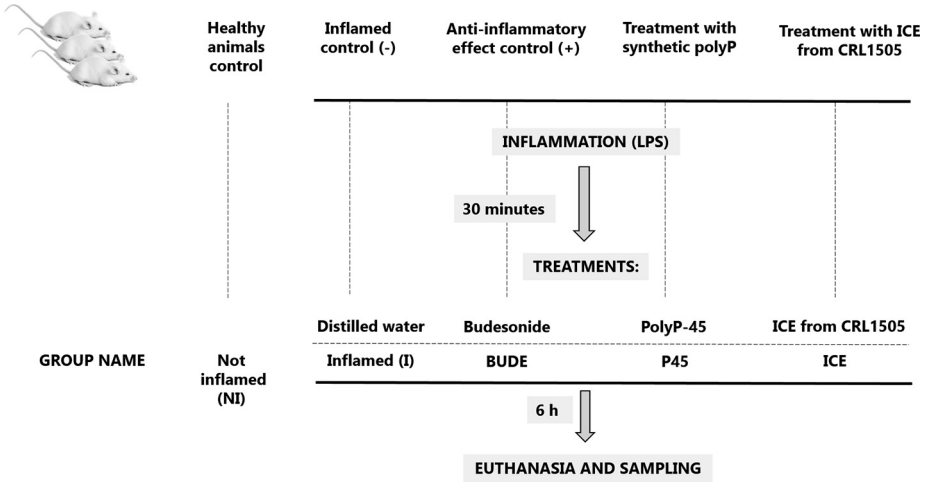

Fig. 1. Experimental protocol used in this work. Male 6-wk-old Swiss albino mice received nasally lipopolysaccharide (LPS) from *Escherichia coli* O55: B5 (200 mg/kg). They were randomized into four groups to receive the different nasal treatments at 30 min after the inflammatory challenge: distillated water (inflamed control, I group), budesonide (5.6 μg/mL) (BUDE group), synthetic polyP (P45 group) or ICE from CRL1505 (ICE group). Healthy animals that not receive the treatment with LPS were used as healthy control (not inflamed control, NI group). Samples were obtained at 6 h post-administration of LPS. Six animals per groups were used in the experiments.

cate using cDNA (60 ng), the primer (1 μM each), the reaction mixture (1×) for PCR (Green GoTaq® Reaction Buffer Promega, Buenos Aires, Argentina), and 0.1 μL of the enzyme GoTaq® DNA Polymerase (Promega, Buenos Aires, Argentina), final volume of 12.5 μL per reaction. The following controls were included for each sample: a non-template control (without cDNA), a positive control represented by the invariable expression of the 16S rDNA gen, and a positive control for each primer using the genomic DNA as a template. The PCR conditions were: initially, 4 min/95 °C, 30 cycles consisting of 30 s/95 °C, 30 s/50 °C, 60 s/72 °C followed by a final extension at 72 °C for 5 min. The PCR products were separated on 1.5% (w/v) agarose gel at 90 V in 1× TAE buffer (40 mM Tris pH 7.6, 20 mM acetic acid, 1 mM EDTA) and subsequently stained with the solution of Gel Red 0.001% (v/v) (Biotium, Genbiotech, Buenos Aires-Argentina). The gels were photographed using a digital photo documentation system (ChemiDoc XRS +, Biorad, Buenos Aires, Argentina) and analyzed with the Image Lab Software program.

2.6. Experimental model of acute respiratory inflammation

Six-week old Swiss albino male mice were obtained from the closed colony kept at CERELA-CONICET, Tucuman, Argentina. The mice were housed under controlled conditions with 12 h light–dark cycles during the trials. The acute respiratory inflammation was induced in mice by nasal administration of LPS from *Escherichia coli* O55: B5 (Sigma Aldrich-Product No. L2880) at a dose of 200 mg/kg body weight (Griet et al., 2014). The mice were randomized into four groups 30 min after the inflammatory challenge to receive different nasal treatments: 25 μL of distilled water (inflamed control, **I** group); 25 μL of budesonide (5.6 μg/mL) (anti-inflammatory effect, positive control, **BUDE** group); 25 μL of a synthetic polyP (**P45** group), and 25 μL of ICE from CRL1505 (**ICE** group). The experimental model scheme is shown in Fig. 1. Animals without receiving LPS were used as healthy control (not inflamed control, **NI** group). Thirty mice in total were used in the experiment. Samples were obtained after 6 h post-administration of LPS. Animal protocols were approved by the Ethical Animal Protection Committee of CERELA-CONICET, Tucuman, Argentina, under the protocol number LEF-2013–01, and all trials comply with the current laws of Argentina and international organizations for the use of experimental animals.

2.7. Leukocyte counts in blood and bronchoalveolar lavage (BAL)

Blood samples were obtained from ketamine-xylazine-anesthetized animals by cardiac puncture in heparinized tubes. BAL samples were obtained as described previously Kolling et al. (2015). Briefly, the trachea was exposed surgically and incubated with a catheter. A small incision was made in the trachea and 1 mL of sterile PBS with 1% heparin was instilled into the lungs. The recovered fluid was centrifuged at 2500 rpm for 4.5 min. The supernatant was stored at −20 °C and the pellet was used for leukocyte counting according to the conventional hematological methodology. Total numbers of blood and BAL leukocytes were determined with a hemocytometer. Differential cell counts were performed by counting 200 cells in blood and BAL smears stained with May-Grünwald Giemsa using a light microscope (1000×) and absolute cell numbers were calculated (Kolling et al., 2015).

2.8. Concentration of cytokines in BAL and blood

Tumor necrosis factor α (TNF-α), interferon γ (IFN-γ), interleukin (IL) −6, IL-10, IL-17A, IL-4, and IL-2 were determined in

serum and BAL by using commercially available Th1/Th2/Th17 CBA kit (Cytometric Bead Array) following the manufacturer's recommendations (BD™ catalog No. 560485). The concentrations were expressed in picograms (pg)/mL using standard curves.

2.9. Statistical analysis

The data obtained in this work corresponded to at least three independent trials and were reported as mean values ± standard deviation (SD). After verification of the normal distribution of data, the 2-way ANOVA was performed using GraphPad Prism 7. Differences were considered significant with $p < 0.05$.

3. Results

3.1. PolyP accumulation in L. rhamnosus CRL1505

Previous studies (Deza et al., 2017) using transmission electron microscopy and a DAPI-based fluorescence technique put in evidence the accumulation of large amounts of polyP by the immunobiotic *L. rhamnosus* CRL1505 when growing in MCM medium with 9.2 g/L of inorganic phosphate. In this work, polyP was evidenced in CRL1505 strain by specific staining with methylene blue (Neisser staining). In addition, the molecular weight of this polyanion was estimated by electrophoresis in polyacrylamide gels. Fig. 2 shows *L. rhamnosus* CRL1505 cells stained with Neisser's reagent and observed by immersion optical microscopy. PolyP inclusions into the cytoplasm of CRL1505 were visualized as high intensity blackheads.

PAGE was also used to separate and visualize the polyP from ICE of *L. rhamnosus* CRL1505. Fig. 3 shows the electrophoretic runs. The standard polyP 45 (lane 1) used as molecular weight marker was located in the lower area of the gel, while the ICE band (lane 2) was placed in the upper part of the gel suggesting that the CRL1505-polyP chain length is greater than 45 phosphate residues. The polyP bands obtained (synthetic polyp 45 and polyP from ICE) are characteristic of polyP migration in polyacrylamide gels as it was reported (Clark and Wood, 1987; Leitão et al., 1995; Mullan et al., 2002; Smith et al., 2010; Alcántara et al., 2014; Saiki et al., 2016). No band in the line corresponding to the sterile MCM broth (lane 3) was observed indicating absence of interference with the medium components. Likewise, the absence of bands in lane 4 (culture supernatant) indicates that polyP remains inside the cells.

The amount of polyP-ICE (as soluble phosphate) was determined by a spectrophotometric technique adapted for quantification of the phosphate released by hydrolysis of the polyP from CRL 1505. The intracellular phosphate concentration was 3.24 ± 0.06 mg Na_2HPO_4/mL of extract.

From *L. rhamnosus* CRL1505 genome sequence deposited at Genbank (ATBI00000000) was feasible to find out the genes *ppk*, *ppx* and *ppx2* encoding for the enzymes involved in the polyP metabolism: a polyphosphate kinase (PPK) and two exopolyphosphatases (PPX1 and PPX2), respectively. To validate the functionality of these gens, a transcriptional analysis of *L. rhamnosus* CRL1505 was performed. The RT-PCR revealed the presence of *ppk*, *ppx* and *ppx2* transcripts (Fig. 4), in agreement with results obtained by Neisser staining and PAGE that evinced the presence of polyP in CRL1505.

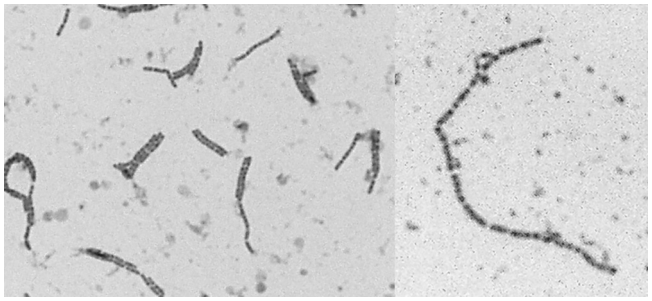

Fig. 2. Optical immersion micrographs (100×) of *L. rhamnosus* CRL1505 grown in MCM (free pH, stationary phase, 37° C) with Neisser staining.

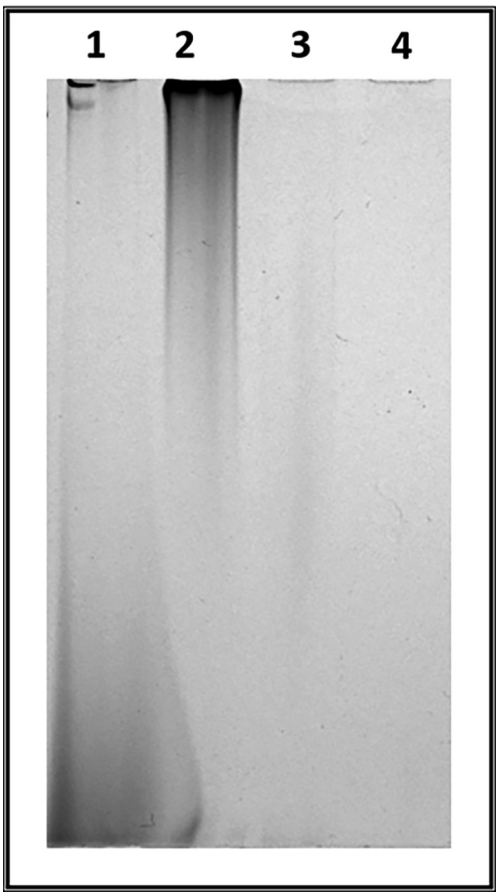

Fig. 3. Analysis by PAGE (4%) of polyP from *L. rhamnosus* CRL1505 grown in MCM (free pH, 37 °C, stationary growth phase). Lines: (1) Molecular size marker (polyP 45); (2); Intracellular extract from CRL1505 (ICE) (3); Sterile culture media (MCM); (4) Culture supernatant from CRL1505 (SN).

3.2. Nasal administration of CRL1505-ICE in LPS-challenged mice

The functionality of the ICE from *L. rhamnosus* CRL1505 containing polyP and the standard polyp 45 was evaluated using a murine model of acute respiratory inflammation induced by LPS (Griet et al., 2014). The pure ICE-CRL1505 with a phosphate concentration of 3.24 ± 0.06 mg Na_2HPO_4/mL was used. In order to define the dose of standard polyP to be administered to the mice, dilutions of this hydrolyzed polyP were quantified as soluble phosphate (Na_2HPO_4). The linearity of the correlation curve obtained (standard polyP concentration vs phosphate concentration) was optimal, with $R^2 = 0.9979$ (Fig. S1). This curve was used to match the phosphate concentration present in the ICE of CRL1505 to a solution of polyP 45. The concentration of standard polyP calculated from the correlation analysis for use in the murine model was 0.57 ± 0.01 mg of polyP 45/mL, equivalent to 3.24 ± 0.06 mg Na_2HPO_4/mL (ICE-CRL1505 concentration).

In the experimental model of acute respiratory inflammation used, local administration of LPS induced a significant ($p < 0.05$)

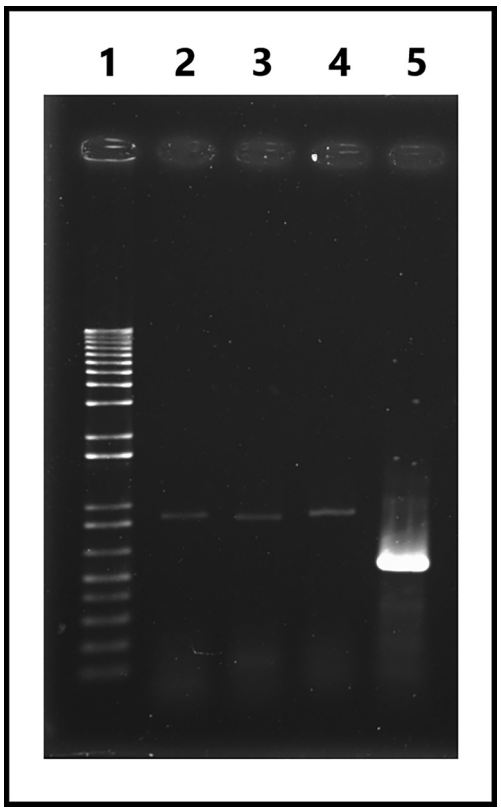

Fig. 4. Agarose gel electrophoresis of amplification products (~900 bp) of the genes *ppk*, *ppx1* and *ppx2* by RT-PCR in *L. rhamnosus* CRL1505. The strain was cultivated in MCM (free pH, stationary growth phase). Lines: (1) Molecular weight marker, (2) *ppx1*, (3) *ppx2*, (4) *ppk*, (5) 16 S rRNA.

increase in the cell counts (leukocytes, macrophages, neutrophils) in BAL of the inflamed group (I group) (Fig. 5). The treatment with ICE, polyP 45 or budesonide significantly reduced these counts in the respiratory tract (41.3–57.2% in macrophages and 90.5–93% in neutrophils) showing values similar to those of normal mice (NI group) (Fig. 5).

Challenge with LPS reduced the number of blood leukocytes in all the experimental groups compared to NI group (Fig. 6). However, only the ICE group showed leukocytes counts significantly ($p < 0.05$) higher compared to I group at 6 h post-challenge, though without reaching values of the NI control group (Fig. 6A). In addition, LPS also decreased significantly the blood neutrophil count ($p < 0.05$) in mice of I group with respect to NI group (Fig. 6B), but treatment with either P45 or ICE produced an increase in neutrophil numbers, which was lower than group NI control.

As shown in Fig. 7, challenge with LPS induced an increase in cytokines (IL-10, IL-17A, TNF-α, IFN-γ, IL-6, IL-4 and IL-2) in both BAL and serum in the I group respect to control mice (NI group), no effect being detected by different the different anti-inflammatory treatments at 6 h post challenge (Fig. 7A). In contrast, at systemic level, treatment with ICE, P45 and BUDE significantly decreased all cytokines levels compared to I group reaching values similar to those of control healthy mice (NI group, Fig. 7B).

4. Discussion

Biologically active components derived from probiotic lactobacilli strains represent the evolution of science in probiotic studies and their applications. In this area, recent studies describe polyP of lactic acid bacteria as a biocomponent responsible for probiotic effects in animal models (Segawa et al., 2011;Tanaka et al., 2015; Kashima et al., 2015; Sakatani et al., 2016). In previous studies we demonstrated that probiotic *L. rhamnosus* CRL1505 accumulates intracellular polyP through transmission electronic microscopy and a DAPI-based fluorescence technique (Deza et al., 2017). In this work, the presence of polyP granules was observed by Neisser's specific staining and optical microscopy, with similar results to those reported for other lactobacilli (Alcántara et al., 2014; Huang et al., 2016). Studies by PAGE indicated that CRL1505 accumulates polyP inside the cell, which would have a chain length greater than 45 phosphate residues (compared to

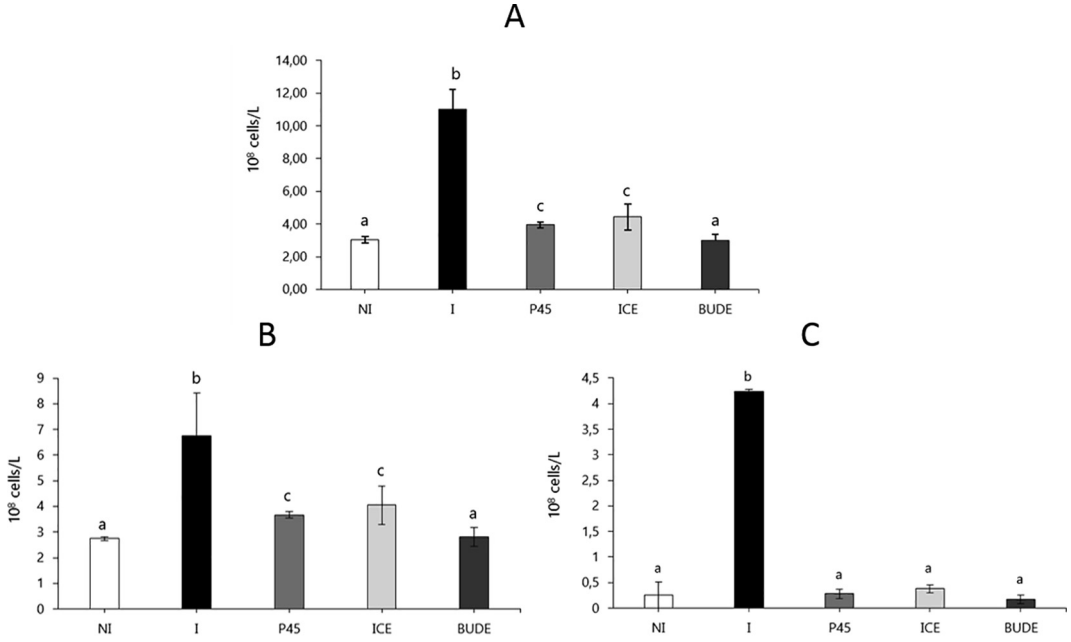

Fig. 5. Total leukocyte counts (A) and counts of macrophages (B) and neutrophils (C) in bronchoalveolar lavage (BAL) at 6 h post LPS-challenge. Mice groups: NI, not inflamed control; I, inflamed control group; BUDE, budesonide group; P45, group treated with PolyP-45; ICE, group treated with ICE from CRL 1505. [a, b, c] Groups with different letter are significantly different ($p < 0.05$).

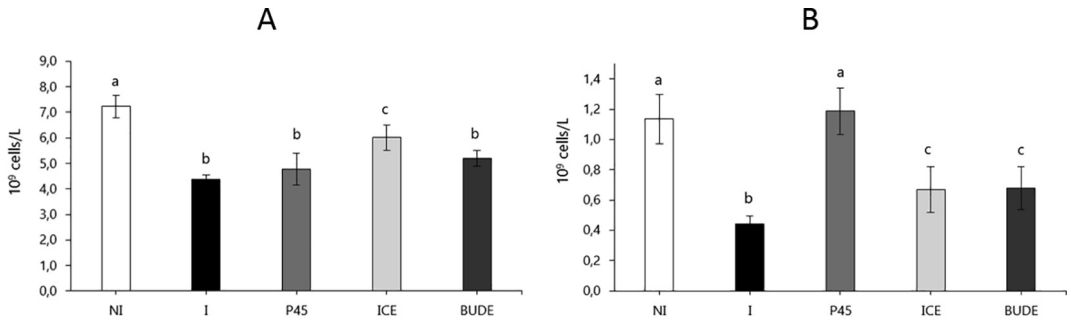

Fig. 6. Total leukocyte counts (A) and neutrophil counts (B) in blood at 6 h post LPS-challenge. Mice groups: NI, not inflamed control; I, inflamed control group; BUDE, budesonide group; P45, group treated with polyP-45; ICE, group treated with ICE from CRL 1505. [a, b, c] Groups with different letter are significantly different ($p < 0.05$).

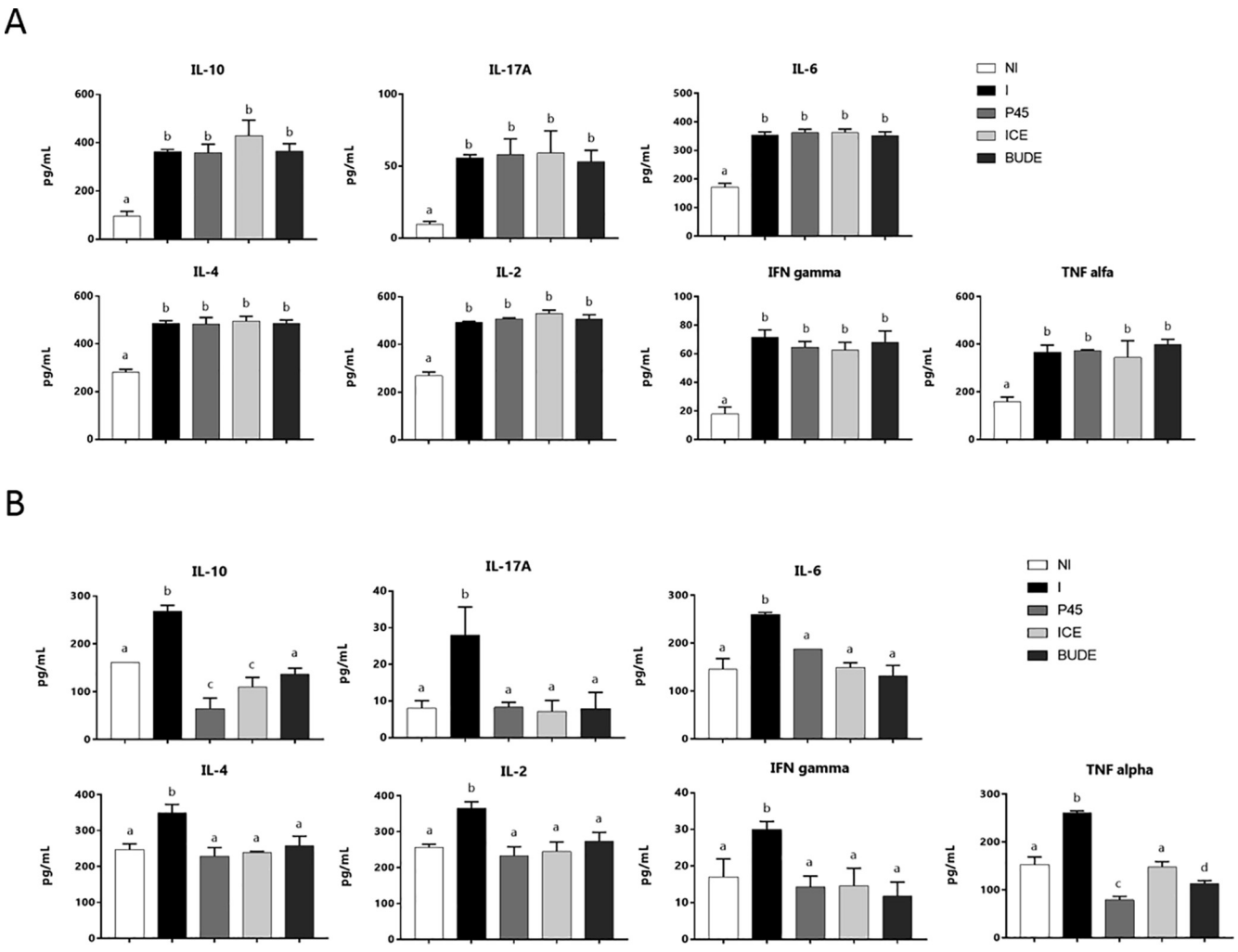

Fig. 7. Cytokine levels in broncho-alveolar lavages (A) and blood (B) at 6 h post LPS-challenge. Mice groups: NI, not inflamed control; I, inflamed control group; BUDE, budesonide group; P45, group treated with polyP-45; ICE, group treated with ICE from CRL 1505. The results represent data from three independent experiments. Results are expressed as mean ± SD. [a,b,c,d] Means in a bar with different letters were significantly different ($p < 0.05$).

polyP 45 used as standard) and it is not excreted. Similar results were reported by Saiki et al. (2016) for the polyP of *L. paracasei* JCM 1163, which has about 700 phosphate residues. In this case, however, polyP was also found in the culture supernatants but in very low quantities (about 1000 times lower than the intracellular content). From this evidence, authors suggest that polyP is not actively excreted but rather it would leak out of the cells.

The polyP accumulation by *L. rhamnosus* CRL1505 was correlated with the presence of *ppk* gene codifying for the enzyme polyphosphate kinase (PPK), the main one involved in the synthesis of polyP (Rao and Kornberg, 1999). The expression of *ppx1* and *ppx2,* also involved in the polyP metabolism, was corroborated by RT-PCR. In CRL1505, *ppk, ppx1* and *ppx2* make up the same operon, so their transcription seems to be co-regulated according to results presented. These results suggest an extra regulation of the PPX enzyme, thus prevailing polyP synthesis and accumulation over its degradation, as in *E. coli* (Kuroda et al., 1997). In this case, both polyP synthesis and degradation, are regulated by guanosine

tetraphosphate (ppGpp) that specifically interacts with PPX inhibiting its activity. In this sense, physiological conditions such as fasting in amino acids, increases the level of ppGpp resulting in polyP accumulation while low levels of ppGpp, as it happens during exponential growth, favors its hydrolysis, thus decreasing intracellular concentration

Quantification of polyP is of primary importance for its potential use as therapeutic agent. For this purpose, a spectrophotometric technique measuring soluble phosphate concentration from hydrolyzed polyP was used. Through this simple and low cost methodology it is possible to quantify polyP in terms of phosphate monomers concentration, as it was previously reported (Mullan et al., 2002; Smith et al., 2010; Segawa et al., 2011). In contrast, the PPK/ATP/luciferase system commonly used for the extraction of polyP and determination of free phosphate released by enzymatic degradation of the polymer (Saiki et al., 2016; Bru et al., 2017) requires considerable investments of money and time. Recently, a streamlined method for polyP quantification in bacteria, using a silica membrane column extraction optimized for rapid processing of multiple samples, digestion of polyP with the polyP-specific exopolyphosphatase ScPPX, and detection of the resulting free phosphate with a sensitive ascorbic acid-based colorimetric assay it was reported (Pokhrel et al., 2019). This procedure is straightforward, inexpensive, and allows reliable polyP quantification in diverse bacterial species.

Recent studies report the anti-inflammatory effect of polyP from different strains of *Lactobacillus* at the intestinal level. In this sense, the polyP of *L. paracasei* JCM 1163 significantly suppresses the oxidant-induced intestinal permeability in mouse small intestine enhancing intestinal barrier functions (Saiki et al., 2016). Besides, other researchers reported that the polyP of *L. brevis* SBC 8803 improves the intestinal barrier (Segawa et al., 2011; Tanaka et al., 2015), suppresses inflammation and intestinal fibrosis (Kashima et al., 2015) and even induces apoptosis and inhibits the progression of colon cancer cells through the activation of ERK signaling (Sakatani et al., 2016). This group proposes *L. brevis* SBC8803-derived polyP as an antitumor drug with fewer side effects than conventional drugs. However, there is no background in the literature about the administration of probiotic-derived polyP by a route other than oral, such as the intranasal route, to evaluate polyP effects on another mucosa such as the respiratory mucosa. In this regard, different experimental models of pulmonary inflammation were used to understand the mechanisms of lung damage and test new therapeutic strategies (Matute-Bello et al., 2008; Aeffner et al., 2015; Kumar et al., 2016; Chen et al., 2017). In the present study, a model of acute respiratory inflammation induced by intranasal administration of LPS was used (Griet et al., 2014) which is an agonist of TLR4 (Atabai and Matthay, 2002). It is known that inhibition of pro-inflammatory cytokine production, cellular apoptosis, and NF-kB activation after LPS challenge reduces lung injuries and improves survival rate (Griet et al., 2014; Chen et al., 2017).

In this study, the protection against LPS-induced acute respiratory inflammation in mice by intranasal treatment of cell free extract of *L. rhamnosus* CRL1505 containing polyP is reported for the first time. Gram-negative bacterial cell wall component, LPS, is a typical immunomodulatory molecule that causes inflammation and neutrophil recruitment (Hayashi et al., 2003; Reber et al., 2017). In our model, LPS inhalation elicits pulmonary inflammation such as acute injury, which occurs after 1–3 h and reaches a maximum at 6 h (Griet et al., 2014). At this point, the neutrophils and macrophages are induced to migrate to the pulmonary space. The pro-inflammatory cytokines produced by these macrophages recruited and activated neutrophils, which adhered to the endothelium of affected capillaries and migrated to air spaces. Also, a reduction in the macrophages and neutrophils numbs in peripheral blood, and an increase in the level of IL-10, IL-17, IL-6, IL-2, IL-4, INF-γ and TNF-α locally and in blood was observed. These findings are consistent with studies previously reported in animal models (de Oliveira et al., 2008; Matthay and Howard, 2012; Griet et al., 2014; Lee et al., 2014) as well as in several clinical studies (Soromou et al., 2012) where the accumulation of neutrophils in the alveolar spaces contributed to inflammation and cytotoxic effects on the lung cells.

At present, glucocorticoids are the most frequently used anti-inflammatory drugs for clinical treatment of respiratory inflammation. In this study, budesonide was used as positive control of anti-inflammatory efficiency and compared with polyP (ICE and 45) in LPS-induced respiratory inflammation. Our results were in line with the findings of Mokra et al. (2016). Authors showed that the intratracheal treatment with budesonide reduced lung edema, cell infiltration into the lung and apoptosis of epithelial cells, and decreased concentrations of pro-inflammatory markers (IL-1β, IL-6, IL-8, TNF-α, IFN-γ, esRAGE, caspase-3) in lung and blood, thus resulting in improved ventilation (Gao and Ju, 2016; Ju et al., 2016)

Therefore, we carefully studied the effect of ICE of *L. rhamnosus* CRL1505 containing polyP in the mouse model for acute respiratory inflammation induced by intranasal instillation of LPS in hopes of establishing a potential compound against respiratory inflammation. Intranasal treatment with ICE and synthetic polyP (P45) decreased total cells number of neutrophils and macrophages in BAL compared with I group. The reduction in leukocyte migration to the bronchoalveolar space it was associated with the normalization of the number of neutrophils in peripheral blood. Activated macrophages derived pro-inflammatory cytokines play critical roles in inflammatory diseases (Huang et al., 2014) and since they produced acute lung injury (Lee et al., 2014). In this work, increased levels of all cytokines were observed in BAL at 6 h post-challenge without obtaining significant differences between the treatment groups (BUDE, P45 and ICE) and the inflammation control (I group). However, the level of cytokines pro-inflammatory such as IL-17, IL-6, IL-2, IL-4, INF-γ in serum was normalized by polyP (ICE, 45) and budesonide, without differences among them. On the other hand, only the ICE treatment was able to normalize serum TNF-α levels unlike polyP 45 and budesonide groups, which showed values lower than the healthy group (NI group). The anti-inflammatory effect of polyP was also evinced in other experimental models. The intrarectal administration of polyP from *L. brevis* SBC8803 in a murine model of acute colitis significantly improved the survival rate and reduced intestinal injury by suppressing the production of pro-inflammatory cytokines such as IL-1β and IL-6 (Segawa et al., 2011). Using the same animal model, Kashima et al. (2015) reported a significant decrease in mRNA expression levels of IL-1β, TNF-α and IFN-γ in mice treated with a synthetic polyP. In our study, the therapeutic treatment with ICE polyP or budesonide normalized the serum levels of IL-10, unlike the synthetic polyP that showed lower values than the healthy animals. It is known that IL-10 has an important protective role in the control of immunopathology during respiratory infections (Villena et al., 2012a; Chiba et al., 2013) and acute respiratory damage (Hiroshima et al., 2014; Wu et al., 2014) contributing to the restitution of the balance between pro-inflammatory and anti-inflammatory factors. These results suggest that the suppression of inflammation in the lung by ICE polyP is associated with the inhibition of pro-inflammatory cytokine release.

5. Conclusion

In summary, polyP is a common product of lactobacilli and other bacteria. As fast as we know, this is the first report concerning the anti-inflammatory effect in the respiratory tract by intrana-

sal administration of ICE of CRL1505 containing polyP. In this way, ICE with polyP was able to prevent the development of a local inflammatory response in the respiratory mucosa in a murine model of acute respiratory inflammation. Although several probiotic lactic acid bacteria with anti-inflammatory properties are known, few biomolecules derived from them have been identified and evaluated (Griet et al., 2014). The properties described for this new bioactive agent, the polyP of the immunobiotic CRL1505, support the search for biological alternatives to mitigate inflammatory disorders of the respiratory tract, which represents a public health problem like Covid-19. More comprehensive studies are still required for clinical applications of this bioactive agent.

Declaration of Competing Interest

The authors declare that they have no known competing financial interests or personal relationships that could have appeared to influence the work reported in this paper.

Acknowledgments

The authors acknowledge the financial support of the Consejo Nacional de Investigaciones Científicas y Técnicas (CONICET) and Agencia Nacional de Promoción Científica y Tecnológica (ANPCyT, PICT2017-786).

Appendix A. Supplementary material

Supplementary data to this article can be found online at https://doi.org/10.1016/j.sjbs.2021.06.010.

References

Aeffner, F., Bolon, B., Davis, I.C., 2015. Mouse models of acute respiratory distress syndrome: a review of analytical approaches, pathologic features, and common measurements. Toxicol. Pathol. 43 (8), 1074–1092.

Alcántara, C., Blasco, A., Zúñiga, M., Monedero, V., 2014. Accumulation of polyphosphate in Lactobacillus spp. and its involvement in stress resistance. Appl. Environ. Microbiol. 80 (5), 1650–1659.

Atabai, K., Matthay, M., 2002. The pulmonary physician in critical care• 5: acute lung injury and the acute respiratory distress syndrome: definitions and epidemiology. Thorax 57 (5), 452–458.

Bru, S., Jiménez, J., Canadell, D., Ariño, J., Clotet, J., 2017. Improvement of biochemical methods of polyP quantification. Microbial Cell. 4 (1), 6.

Clark, J.E., Wood, H.G., 1987. Preparation of standards and determination of sizes of long-chain polyphosphates by gel electrophoresis. Anal. Biochem. 161 (2), 280–290.

Clua, P., Kanmani, P., Zelaya, H., Tada, A., Kober, A., Salva, S., Alvarez, S., Kitazawa, H., Villena, J., 2017. Peptidoglycan from Immunobiotic *Lactobacillus rhamnosus* improves resistance of infant mice to respiratory syncytial viral infection and secondary pneumococcal pneumonia. Front. Immunol. 8, 948.

Chen, J.-J., Huang, C.-C., Chang, H.-Y., Li, P.-Y., Liang, Y.-C., Deng, J.-S., Huang, S.-S., Huang, G.-J., 2017. *Scutellaria baicalensis* ameliorates acute lung injury by suppressing inflammation *in vitro* and *in vivo*. Am. J. Chin. Med. 45 (01), 137–157.

Chiba, E., Tomosada, Y., Vizoso-Pinto, M.G., Salva, S., Takahashi, T., Tsukida, K., Kitazawa, H., Alvarez, S., Villena, J., 2013. Immunobiotic *Lactobacillus rhamnosus* improves resistance of infant mice against respiratory syncytial virus infection. Int. Immunopharmacol. 17 (2), 373–382.

De Angelis, M., Gallo, G., Corbo, M.R., McSweeney, P.L., Faccia, M., Giovine, M., Gobbetti, M., 2003. Phytase activity in sourdough lactic acid bacteria: purification and characterization of a phytase from *Lactobacillus sanfranciscensis* CB1. Int. J. Food Microbiol. 87 (3), 259–270.

de Oliveira, A.L., Lazzarini, R., Cavriani, G., Quinteiro-Filho, W., de Lima, W.T., Palermo-Neto, J., 2008. Effects of single or repeated amphetamine treatment and withdrawal on lung allergic inflammation in rats. Int. Immunopharmacol. 8 (9), 1164–1171.

Deza, M.A.C., Grillo-Puertas, M., Salva, S., Rapisarda, V.A., Gerez, C.L., de Valdez, G.F., 2017. Inorganic salts and intracellular polyphosphate inclusions play a role in the thermotolerance of the immunobiotic *Lactobacillus rhamnosus* CRL 1505. PLoS ONE 12 (6), e0179242.

Dumas, A., Bernard, L., Poquet, Y., Lugo-Villarino, G., Neyrolles, O., 2018. The role of the lung microbiota and the gut–lung axis in respiratory infectious diseases. Cell. Microbiol. 20 (12), e12966.

Ewaschuk, J.B., Diaz, H., Meddings, L., Diederichs, B., Dmytrash, A., Backer, J., Looijer-van Langen, M., Madsen, K.L., 2008. Secreted bioactive factors from Bifidobacterium infantis enhance epithelial cell barrier function. Am. J. Physiol.-Gastrointestinal Liver Physiol. 295 (5), G1025–G1034.

Gao, W., Ju, Y.-n., 2016. Budesonide attenuates ventilator-induced lung injury in a rat model of inflammatory acute respiratory distress syndrome. Arch. Med. Res. 47 (4), 275–284.

Griet, M., Zelaya, H., Mateos, M.V., Salva, S., Juarez, G.E., de Valdez, G.F., Villena, J., Salvador, G.A., Rodriguez, A.V., 2014. Soluble factors from *Lactobacillus reuteri* CRL1098 have anti-inflammatory effects in acute lung injury induced by lipopolysaccharide in mice. PLoS ONE 9 (10), e110027.

Gurr, E., 1965. The rational use of dyes in biology and general staining methods. The rational use of dyes in biology and general staining methods.

Hayashi, F., Means, T.K., Luster, A.D., 2003. Toll-like receptors stimulate human neutrophil function. Blood 102 (7), 2660–2669.

Herrera, M., Salva, S., Villena, J., Barbieri, N., Marranzino, G., Alvarez, S., 2014. Dietary supplementation with *Lactobacilli* improves emergency granulopoiesis in protein-malnourished mice and enhances respiratory innate immune response. PLoS ONE 9 (4), e90227.

Heuvelin, E., Lebreton, C., Grangette, C., Pot, B., Cerf-Bensussan, N., Heyman, M., 2009. Mechanisms involved in alleviation of intestinal inflammation by *Bifidobacterium breve* soluble factors. PLoS ONE 4 (4), e5184.

Hiroshima, Y., Hsu, K., Tedla, N., Chung, Y.M., Chow, S., Herbert, C., Geczy, C.L., 2014. S100A8 induces IL-10 and protects against acute lung injury. J. Immunol. 1302556.

Huang, S., Rabah, H., Jardin, J., Briard-Bion, V., Parayre, S., Maillard, M.-B., Le Loir, Y., Chen, X.D., Schuck, P., Jeantet, R., 2016. Hyperconcentrated sweet whey: a new culture medium that enhances *Propionibacterium freudenreichii* stress tolerance. Applied and environmental microbiology. Appl. Environ. Microbiol. 00748–00716.

Huang, T.-T., Lai, H.-C., Chen, Y.-B., Chen, L.-G., Wu, Y.-H., Ko, Y.-F., Lu, C.-C., Chang, C.-J., Wu, C.-Y., Martel, J., 2014. cis-Resveratrol produces anti-inflammatory effects by inhibiting canonical and non-canonical inflammasomes in macrophages. Innate Immun. 20 (7), 735–750.

Ju, Y.-N., Yu, K.-J., Wang, G.-N., 2016. Budesonide ameliorates lung injury induced by large volume ventilation. BioMed Central Pulmon. Med. 16 (1), 90.

Kashima, S., Fujiya, M., Konishi, H., Ueno, N., Inaba, Y., Moriichi, K., Tanabe, H., Ikuta, K., Ohtake, T., Kohgo, Y., 2015. Polyphosphate, an active molecule derived from probiotic *Lactobacillus brevis*, improves the fibrosis in murine colitis. Trans. Res. 166 (2), 163–175.

Kitazawa, H., Villena, J., 2014. Modulation of respiratory TLR3-anti-viral response by probiotic microorganisms: lessons learned from *Lactobacillus rhamnosus* CRL1505. Front. Immunol. 5, 201.

Kolling, Y., Salva, S., Villena, J., Marranzino, G., Alvarez, S., 2015. Non-viable immunobiotic *Lactobacillus rhamnosus* CRL1505 and its peptidoglycan improve systemic and respiratory innate immune response during recovery of immunocompromised-malnourished mice. Int. Immunopharmacol. 25 (2), 474–484.

Kumar, R.K., Herbert, C., Foster, P.S., 2016. Mouse models of acute exacerbations of allergic asthma. Respirology 21 (5), 842–849.

Kuroda, A., Murphy, H., Cashel, M., Kornberg, A., 1997. Guanosine tetra-and pentaphosphate promote accumulation of inorganic polyphosphate in *Escherichia coli*. J. Biol. Chem. 272 (34), 21240–21243.

Lee, C.-Y., Yang, J.-J., Lee, S.-S., Chen, C.-J., Huang, Y.-C., Huang, K.-H., Kuan, Y.-H., 2014. Protective effect of Ginkgo biloba leaves extract, EGb761, on endotoxin-induced acute lung injury via a JNK-and Akt-dependent NFκB pathway. J. Agric. Food. Chem. 62 (27), 6337–6344.

Leitão, J.M., Lorenz, B., Bachinski, N., Wilhelm, C., Müller, W.E., Schröder, H.C., 1995. Osmotic-stress-induced synthesis and degradation of inorganic polyphosphates in the alga *Phaeodactylumtricornutum*. Mar. Ecol. Prog. Ser. 121, 279–288.

Libertucci, J., Young, V.B., 2019. The role of the microbiota in infectious diseases. Nat. Microbiol. 4 (1), 35.

Liu, Y., Tran, D.Q., Rhoads, J.M., 2018. Probiotics in disease prevention and treatment. J. Clin. Pharmacol. 58, S164–S179.

Markowicz, C., Kubiak, P., Grajek, W., Schmidt, M.T., 2015. Inactivation of *Lactobacillus rhamnosus* GG by fixation modifies its probiotic properties. Can. J. Microbiol. 62 (1), 72–82.

Matthay, M.A., Howard, J.P., 2012. Progress in modelling acute lung injury in a pre-clinical mouse model. Eur. Respiratory Soc., 1062–1063

Matute-Bello, G., Frevert, C.W., Martin, T.R., 2008. Animal models of acute lung injury. Am. J. Physiol.-Lung Cell. Mole. Physiol. 295 (3), L379–L399.

Menard, S., Candalh, C., Bambou, J., Terpend, K., Cerf-Bensussan, N., Heyman, M., 2004. Lactic acid bacteria secrete metabolites retaining anti-inflammatory properties after intestinal transport. Gut 53 (6), 821–828.

Mokra, D., Kosutova, P., Balentova, S., Adamkov, M., Mikolka, P., Mokry, J., Antosova, M., Calkovska, A., 2016. Effects of budesonide on the lung functions, inflammation and apoptosis in a saline-lavage model of acute lung injury. J. Physiol. Pharmacol. 67, 919–932.

Mullan, A., Quinn, J.P., McGrath, J.W., 2002. A nonradioactive method for the assay of polyphosphate kinase activity and its application in the study of polyphosphate metabolism in *Burkholderia cepacia*. Anal. Biochem. 308 (2), 294–299.

Petrof, E.O., Claud, E.C., Sun, J., Abramova, T., Guo, Y., Waypa, T.S., He, S.-M., Nakagawa, Y., Chang, E.B., 2009. Bacteria-free solution derived from *Lactobacillus plantarum* inhibits multiple NF-kappaB pathways and inhibits proteasome function. Inflamm. Bowel Dis. 15 (10), 1537–1547.

Pokhrel, A., Lingo, J.C., Wolschendorf, F., Gray, M.J., 2019. Assaying for inorganic polyphosphate in Bacteria. J. Visual. Exp. 143, e58818.

Rao, N., Kornberg, A., 1999. Inorganic polyphosphate regulates responses of Escherichia coli to nutritional stringencies, environmental stresses and survival in the stationary phase. In: Inorganic Polyphosphates. Springer, pp 183–195.

Raya, R., Bardowski, J., Andersen, P.S., Ehrlich, S.D., Chopin, A., 1998. Multiple transcriptional control of the *Lactococcus lactis* trp operon. J. Bacteriol. 180 (12), 3174–3180.

Reber, L.L., Gillis, C.M., Starkl, P., Jönsson, F., Sibilano, R., Marichal, T., Gaudenzio, N., Bérard, M., Rogalla, S., Contag, C.H., 2017. Neutrophil myeloperoxidase diminishes the toxic effects and mortality induced by lipopolysaccharide. J. Exp. Med. 214 (5), 1249–1258.

Saiki, A., Ishida, Y., Segawa, S., Hirota, R., Nakamura, T., Kuroda, A., 2016. A *Lactobacillus mutant* capable of accumulating long-chain polyphosphates that enhance intestinal barrier function. Biosci. Biotechnol. Biochem. 80 (5), 955–961.

Sakatani, A., Fujiya, M., Ueno, N., Kashima, S., Sasajima, J., Moriichi, K., Ikuta, K., Tanabe, H., Kohgo, Y., 2016. Polyphosphate derived from *Lactobacillus brevis* inhibits colon cancer progression through induction of cell apoptosis. Anticancer Res. 36 (2), 591–598.

Salva, S., Villena, J., Alvarez, S., 2010. Immunomodulatory activity of *Lactobacillus rhamnosus* strains isolated from goat milk: impact on intestinal and respiratory infections. Int. J. Food Microbiol. 141 (1–2), 82–89.

Segawa, S., Fujiya, M., Konishi, H., Ueno, N., Kobayashi, N., Shigyo, T., Kohgo, Y., 2011. Probiotic-derived polyphosphate enhances the epithelial barrier function and maintains intestinal homeostasis through integrin–p38 MAPK pathway. PLoS ONE 6 (8), e23278.

Smith, S.A., Choi, S.H., Davis-Harrison, R., Huyck, J., Boettcher, J., Rienstra, C.M., Morrissey, J.H., 2010. Polyphosphate exerts differential effects on blood clotting, depending on polymer size. Blood. blood-2010-2001-266791.

Soromou, L.W., Chu, X., Jiang, L., Wei, M., Huo, M., Chen, N., Guan, S., Yang, X., Chen, C., Feng, H., 2012. *In vitro* and *in vivo* protection provided by pinocembrin against lipopolysaccharide-induced inflammatory responses. Int. Immunopharmacol. 14 (1), 66–74.

Tanaka, K., Fujiya, M., Konishi, H., Ueno, N., Kashima, S., Sasajima, J., Moriichi, K., Ikuta, K., Tanabe, H., Kohgo, Y., 2015. Probiotic-derived polyphosphate improves the intestinal barrier function through the caveolin-dependent endocytic pathway. Biochem. Biophys. Res. Commun. 467 (3), 541–548.

Tomosada, Y., Chiba, E., Zelaya, H., Takahashi, T., Tsukida, K., Kitazawa, H., Alvarez, S., Villena, J., 2013. Nasally administered *Lactobacillus rhamnosus* strains differentially modulate respiratory antiviral immune responses and induce protection against respiratory syncytial virus infection. BioMed Central Immunol. 14 (1), 40.

Tonetti, F.R., Islam, M.A., Vizoso-Pinto, M.G., Takahashi, H., Kitazawa, H., Villena, J., 2020. Nasal priming with immunobiotic *lactobacilli* improves the adaptive immune response against influenza virus. Int. Immunopharmacol. 78, 106115.

Villena, J., Barbieri, N., Salva, S., Herrera, M., Alvarez, S., 2009. Enhanced immune response to *pneumococcal* infection in malnourished mice nasally treated with heat-killed *Lactobacillus casei*. Microbiol. Immunol. 53 (11), 636–646.

Villena, J., Chiba, E., Tomosada, Y., Salva, S., Marranzino, G., Kitazawa, H., Alvarez, S., 2012a. Orally administered *Lactobacillus rhamnosus* modulates the respiratory immune response triggered by the viral pathogen-associated molecular pattern poly (I: C). BioMed Central Immunol. 13 (1), 53.

Villena, J., Salva, S., Núñez, M., Corzo, J., Tolaba, R., Faedda, J., Font, G., Alvarez, S., 2012b. Probiotics for everyone! The novel immunobiotic *Lactobacillus rhamnosus* CRL1505 and the beginning of Social Probiotic Programs in Argentina. Int. J. Biotechnol. Wellness Ind. 1 (3), 189–198.

Villena, J., Vizoso-Pinto, M.G., Kitazawa, H., 2016. Intestinal innate antiviral immunity and immunobiotics: beneficial effects against rotavirus infection. Front. Immunol. 7, 563.

Wu, Q., Li, R., Soromou, L.W., Chen, N., Yuan, X., Sun, G., Li, B., Feng, H., 2014. p-Synephrine suppresses lipopolysaccharide-induced acute lung injury by inhibition of the NF-κB signaling pathway. Inflamm. Res. 63 (6), 429–439.

Yan, F., Cao, H., Cover, T.L., Whitehead, R., Washington, M.K., Polk, D.B., 2007. Soluble proteins produced by probiotic bacteria regulate intestinal epithelial cell survival and growth. Gastroenterology 132 (2), 562–575.

Zelaya, H., Alvarez, S., Kitazawa, H., Villena, J., 2016. Respiratory antiviral immunity and immunobiotics: beneficial effects on inflammation-coagulation interaction during influenza virus infection. Front. Immunol. 7, 633.

Zelaya, H., Tada, A., Vizoso-Pinto, M.G., Salva, S., Kanmani, P., Agüero, G., Alvarez, S., Kitazawa, H., Villena, J., 2015. Nasal priming with immunobiotic *Lactobacillus rhamnosus* modulates inflammation–coagulation interactions and reduces influenza virus-associated pulmonary damage. Inflamm. Res. 64 (8), 589–602.

Zelaya, H., Tsukida, K., Chiba, E., Marranzino, G., Alvarez, S., Kitazawa, H., Agüero, G., Villena, J., 2014. Immunobiotic *lactobacilli* reduce viral-associated pulmonary damage through the modulation of inflammation–coagulation interactions. Int. Immunopharmacol. 19 (1), 161–173.